processes

MDPI

Article

Comparative Analysis of Microscopic Pore Throat Heterogeneity in the Chang 6 Tight Sandstone Reservoir: Implications for Production Dynamics and Development Strategies in the Wuqi-Dingbian Region, Ordos Basin

Jun Li [1], Mingwei Wang [2,*], Yan Li [1], Kaitao Yuan [1], Liang Liu [1] and Lingdong Meng [3]

[1] Dingbian Oil Production Plant of Yanchang Oilfield Company, Yulin 718600, China; lj_15249011188@sina.com (J.L.); ly_zckfk88@sina.com (Y.L.); ykt_zckfkkfs@sina.com (K.Y.); ll_kfk@sina.com (L.L.)
[2] School of Oil & Natural Gas Engineering, Southwest Petroleum University, Chengdu 610500, China
[3] School of Earth Sciences, Northeast Petroleum University, Daqing 163318, China; menglingdong001@163.com
* Correspondence: tougaozhongwen@163.com

Abstract: This study systematically investigates the heterogeneity of the Chang 6 reservoir in the Wuqi–Dingbian region of the Ordos Basin through integrated petrographic analysis using scanning electron microscopy (SEM), thin-section petrography, and mercury intrusion porosimetry. The results reveal that this feldspathic sandstone reservoir exhibits significant compositional and textural variations controlled by depositional environments. Dingbian samples displayed elevated feldspar (avg. 42.3%), lithic fragments (18.1%), and carbonate cementation (15.7%), accompanied by intense mechanical compaction and cementation processes. Pore systems in Dingbian were dominated by residual intergranular pores (58–62% of total porosity) and secondary dissolution pores. In contrast, Wuqi reservoirs demonstrated superior pore connectivity through well-developed intergranular pores (65–72%), grain boundary pores, and microfracture networks. Pore throat characterization revealed distinct architectural patterns: Wuqi exhibited broad bimodal/multimodal distributions (0.1–50 μm) with 35–40% macro-throat (>10 μm) contribution to flow capacity, while Dingbian showed narrow unimodal distributions (1–10 μm) with <15% macro-throat participation. These microstructural divergences fundamentally governed contrasting production behaviors. Wuqi wells achieved higher initial flow rates (15–20 m^3/d) with 60–70% water cut, yet maintained stable production through effective displacement systems enabled by dominant macropores. Conversely, Dingbian wells produced lower yields (5–8 m^3/d) with 75–85% water cut, experiencing rapid 30–40% initial declines that transitioned to prolonged low-rate production phases. This petrophysical framework provides critical insights for optimized development strategies in heterogeneous tight sandstone reservoirs, particularly regarding water management and enhanced oil recovery potential.

Keywords: Ordos Basin; reservoir characteristics; pore throat structure; capillary pressure; provenance system

check for updates

Academic Editor: Qingbang Meng

Received: 13 March 2025
Revised: 3 April 2025
Accepted: 4 April 2025
Published: 7 April 2025

Citation: Li, J.; Wang, M.; Li, Y.; Yuan, K.; Liu, L.; Meng, L. Comparative Analysis of Microscopic Pore Throat Heterogeneity in the Chang 6 Tight Sandstone Reservoir: Implications for Production Dynamics and Development Strategies in the Wuqi-Dingbian Region, Ordos Basin. *Processes* **2025**, *13*, 1109. https://doi.org/10.3390/pr13041109

Copyright: © 2025 by the authors. Licensee MDPI, Basel, Switzerland. This article is an open access article distributed under the terms and conditions of the Creative Commons Attribution (CC BY) license (https://creativecommons.org/licenses/by/4.0/).

1. Introduction

Tight sandstone reservoirs have emerged as a crucial unconventional resource in global energy supply, accounting for over 40% of newly discovered hydrocarbon reserves in continental basins during the past decade (Zou et al., 2022) [1]. The Ordos Basin in North China, as the second-largest sedimentary basin in China, contains extensive Triassic tight

oil resources estimated at 15–20 billion barrels within the Yanchang formation (Yao et al., 2013) [2]. This lacustrine-dominated succession has attracted significant research attention due to its complex depositional architecture and heterogeneous reservoir properties (Sun et al., 2024) [3].

Globally, tight sandstone reservoir characterization has evolved through three developmental phases: (1) initial recognition of unconventional potential (pre-2000), (2) the technological breakthrough phase (2000–2015), driven by horizontal drilling and hydraulic fracturing, and (3) the precision development phase (post-2015), emphasizing the understanding of reservoir heterogeneity (Law and Curtis, 2002; Clarkson et al., 2011) [4,5]. In China, the Ordos Basin has served as a natural laboratory for tight oil research, with the Yanchang Formation's depositional systems being systematically studied through integrated sedimentological and geochemical approaches (Sun et al., 2024) [6].

The Ordos Basin Triassic Yanchang formation comprises detrital rock deposits from an inland lake basin, which is further divided into 10 oil-bearing formations in descending order. Among these, the deposition periods of Chang 10 to Chang 7 represent lake-prograding phases, while those of Chang 6 to Chang 2 signify lake-retreating stages. The deposition period of Chang 1 corresponds to a quasi-plainification phase [7,8]. The Wu–Ding area is situated in the midwestern part of the Ordos Basin and serves as one of the primary development areas for the Yanchang Oilfield. Over 70% of the total oil production in the Yanchang Oilfield comes from this area, with the Chang 6 oil-bearing formation being a key reservoir system. In this region, during the sedimentation period of Chang 6, a lake-controlled delta-type mudstone system was predominantly formed and influenced by two sediment sources from northwest and northeast directions; consequently, striped distribution patterns are observed within sand bodies [9,10].

The Chang 6 reservoir in the Wu–Ding area represents a typical tight sandstone system with an average porosity of 8.2% and a permeability of <0.3 mD. Recent studies have revealed that its reservoir quality is controlled by three key factors: (1) sedimentary microfacies distribution, (2) diagenetic alteration history, and (3) source rock–reservoir coupling relationships (Wei et al., 2022; Gao et al., 2022; Mahmoodabadi, 2023) [11–13]. The dual-provenance system from northwest and northeast directions creates distinct sandbody architectures, with NE-derived sandstones showing 15–20% higher oil saturation compared to their NW counterparts (Tong et al., 2023) [14]. Advanced characterization techniques have significantly enhanced reservoir understanding. Micro-CT scanning has identified three pore types: residual intergranular pores (42%), dissolution pores (35%), and microfractures (23%) (Yao et al., 2023) [15]. High-pressure mercury injection tests have revealed bimodal pore throat distributions with dominant throat radii of 0.1–1 μm (Zhao et al., 2022) [16]. However, critical knowledge gaps remain regarding source rock influences on reservoir diagenesis—particularly how organic acid generation from different source kitchens modifies pore systems (Guan et al., 2017) [17].

Recent advancements in understanding the control mechanisms of provenance differentiation on reservoir diagenetic evolution have yielded significant breakthroughs [18,19]. Zhao et al. (2023) further developed mineral composition–pore network evolution models using SEM-CT tomography [20]. Zhang et al. (2024) revealed a significantly higher microfracture connectivity index in volcanic lithic sandstones compared to their metamorphic counterparts [21]. Nevertheless, their work insufficiently addressed coupled chemical–mechanical interactions between diagenetic fluids and mineral assemblages. These findings collectively suggest that developing cementation sequence prediction algorithms based on mineralogical composition and implementing geochemistry–rock mechanics cross-scale modeling represent crucial directions for advancing provenance differentiation research.

The regulatory mechanisms of source rock–reservoir coupling effects on reservoir quality have emerged as a critical research frontier [22]. Tohidi et al., 2021 established a quantitative correlation model between source rock maturity (Ro) and the pore structure adjustment coefficient (PSA) through organic acid concentration field modeling and core imbibition experiments [23]. The proposed sweet spot index demonstrates operational efficacy, achieving 78% production compliance in horizontal wells. However, current models have yet to adequately incorporate the kinetic constraints of organic acid migration in overpressured systems. Therefore, coupled pressure–chemical multiphysics simulation represents a critical pathway for advancing source-controlled diagenesis theory.

The fundamental challenge in Wu–Ding's Chang 6 reservoir development lies in understanding source-controlled reservoir heterogeneity. Two critical issues hinder efficient exploitation. Firstly, provenance differentiation impacts the dual-source system and creates mineralogical variations (NW sandstones contain 12–18% volcanic lithics vs. NE's 5–8% metamorphic fragments) that influence diagenetic pathways. Current models insufficiently address how these differences affect cementation patterns and porosity preservation. Secondly, source rock–reservoir coupling mechanism present a challenge; while source rock quality controls hydrocarbon charging efficiency (Guo et al., 2023) [24], its role in diagenetic fluid migration and pore structure modification remains poorly constrained. Organic acids from source rock maturation may create secondary porosity but could also promote authigenic clay growth that reduces permeability [25]. These knowledge gaps lead to suboptimal development strategies, with 30–40% of horizontal wells underperforming predicted rates due to unanticipated reservoir heterogeneity. Existing geological models fail to incorporate source-derived diagenetic effects, resulting in inaccurate sweet spot predictions.

Systematic elucidation remains lacking regarding the quantitative control mechanisms of source rock heterogeneity (e.g., mineralogical composition disparities, sedimentary sorting characteristics) under the dual-provenance system (northwest–northeast sediment supply) on reservoir lithology, pore architecture, and petrophysical parameter variations in the Chang 6 reservoir of the Wu–Ding area, Ordos Basin. Furthermore, the principal geological controls on reservoir heterogeneity necessitate further clarification. This study explored the key role of source rock heterogeneity in shaping the characteristics of the Chang 6 reservoir in the Wu–Ding area through a systematic multi-scale analysis method. The study integrated four workflows to systematically investigate how the spatial variation in source rock characteristics affects reservoir lithology, pore structure, permeability, and production capacity. Through rock mineral composition analysis, quantitative thin-section petrography analysis of rock samples was conducted to distinguish between northwest and northeast sandstone sources and analyze the framework composition, thus achieving provenance discrimination. Scanning electron microscopy–cathodoluminescence imaging was used to reconstruct the diagenetic process, establish a cementation sequence, and constrain oil and gas filling conditions using fluid inclusion micro thermometry. Pore throat distribution mapping was performed through high-pressure mercury injection, mesopore analysis was conducted using nitrogen adsorption, and three-dimensional pore network modeling was performed by combining CT scanning and petrophysical data to characterize the pore system structure. The comprehensive method revealed the systematic relationship between source rock heterogeneity, diagenetic path differentiation, and pore network development, providing key insights for reservoir quality evaluation and productivity optimization in similar lacustrine systems.

2. Sedimentary Petrological Characteristics

Sedimentation plays a pivotal role in geology, influencing not only the scale and rock composition of reservoir development, but also exerting a profound impact on the maturity

and primary pore formation of reservoirs [26–28]. For instance, the Chang 6 reservoir in the Wu–Ding area primarily comprises semi-deep lake and pre-deltaic sediments during its early stages, gradually transitioning to late deltaic foreland sediments. Throughout this process, subaqueous distributary channel sand bodies were extensively developed, predominantly consisting of quartz sandstone interbedded with rock fragment quartz sandstone; the grain size composition mainly comprised fine sandstone and powdery fine sandstone, with grain size increasing gradually from bottom to top. Furthermore, high-magnesium clay, vermiculite, and iron calcite were the principal components in terms of filler material.

Geological studies indicate that the lithological composition types of various source rocks significantly influence the porosity and permeability of sedimentary rock reservoirs (Table 1). In the Dingbian area, these properties are primarily influenced by the northwest source rock, leading to a relatively high content of feldspar and clasts in the detrital component. This condition renders the reservoir more susceptible to compaction, resulting in decreased porosity and permeability. Conversely, in the Wuqi area, it is controlled by the northeast source rock with a shorter transport distance, contributing to better particle roundness compared to the Dingbian area. Furthermore, there is a relative development of chlorite films in the reservoir, which aids in preserving intergranular porosity. Additionally, noticeable carbonate cementation occurs in the Dingbian area, filling remaining intergranular pores and significantly impacting reservoir performance. Conversely, in the Wuqi area, measures have been taken to prevent carbonate cementation formation for preserving intergranular porosity. Overall, sedimentary rock reservoir performance is superior in Wuqi compared to Dingbian.

Table 1. Rock composition Chang 6 reservoir in Wu–Ding area, Ordos Basin.

Area	Quartz (%)	Feldspar (%)	Debris (%)			Components of Interstitial Material (%)								Others (%)	Sample Quantity
			Igneous Debris	Metamorphic Rock Debris	Sedimentary Debris	Kaolinite	Hydromica	Chlorite	Network Clay	Calcite	Iron Calcite	Dolomite	Siliceous		
Wuqi	25.30	45.14	2.50	6.18	1.21	1.55	2.32	3.54	0.27	0.69	2.25	0.64	1.31	7.10	385
Dingbian	31.53	35.49	2.50	6.54	1.71	3.26	1.95	2.92	0.17	0.32	3.77	0.67	1.25	7.93	450
Average	30.04	37.81	2.50	6.45	1.59	2.40	2.14	3.23	0.22	0.50	3.01	0.65	1.28	7.73	835

This study utilizes environmental scanning electron microscopy (ESEM) to characterize the micro-morphology of rock pore structure (Figure 1). This equipment can characterize the microstructure and microtopography of various materials under high or low vacuum conditions, making it an indispensable tool for studying the relationship between the microstructure and properties of various materials. Its secondary electron (SE) imaging resolution in high vacuum mode is 3.0 nm at 30 kV and 8.0 nm at 3 kV.



Figure 1. Environmental scanning electron microscope.

Figure 2a illustrates the presence of a minor amount of autogenous calcite filling within the pores of the Chang 6_1 reservoir rock. In Figure 2b, the bright orange-yellow light indicates the occurrence of calcite replacement and cementation in the Chang 6_2 reservoir

rock. The development of smectite film cementation with well-developed intergranular pores is evident in Figure 2c. Similarly, Figure 2d depicts smectite film cementation and well-developed intergranular pores in the Chang 6_1 reservoir rock. Furthermore, Figure 2e also showcases smectite film cementation along with well-developed intergranular pores in the Chang 6_1 reservoir rock. Moving on to Figure 2f, it reveals that iron calcite, iron kaolinite, and kaolinite predominantly fill most of the pores in the long feldspar component undergoing clastic replacement within the internal structure of the Chang 6_3 reservoir rock; this includes some intergranular pores and clay crystal intercrystalline pores. Microfractures are observed within the Chang 6_1 reservoir as depicted in Figure 2g. Lastly, intracrystalline orientation can be observed for tightly packed grains with some intergranular pores and microfractures within the grains present in Figure 2h.

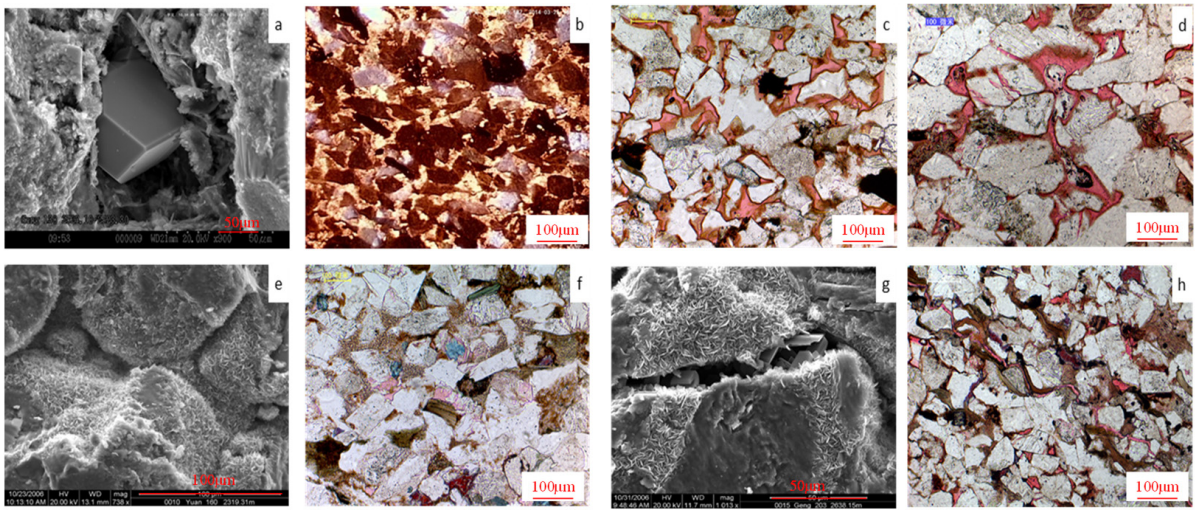


Figure 2. (**a**–**h**) Microscopic images of Chang 6 reservoir in Wu–Ding area, Ordos Basin.

3. Pore Throat Structure and Reservoir Classification Evaluation

3.1. Pore Combination Type

Based on the data obtained from thin sections and scanning electron microscope analysis, it is observed that the primary pore types present in various source rock reservoirs in the Wu–Ding area are residual intergranular pores and dissolution pores (Figure 2c–f), with a minor presence of grain boundary pores and microfractures (Figure 2g,h). The predominant type consists of a combination of dissolution pores–intergranular pores and micro-pores. These diverse pore combinations significantly influence the reservoir properties, with the content of dissolution pores–intergranular pores and micro-pores exerting the most pronounced impact on enhancing reservoir permeability [29]. The total reservoir area ratio in the Wu–Ding area ranges from 0 to 6.54%, averaging at 4.46%. In contrast, the Dingbian area exhibits a total reservoir area ratio ranging from 0 to 6.25%, with an average of 4.18%. Notably, compared to the Dingbian area, the Wu–Ding area demonstrates higher intergranular pore and microfracture contents, which are well developed within the rock matrix, leading to enhanced connectivity and improved fluid permeability (Table 2).

Table 2. Content of pore types in different provenances of Chang 6 reservoir in Wu–Ding area, Ordos Basin.

Area	Intergranular Pore (%)	Emposieu (%)				Intercrystal Pore (%)	Microfracture (%)	Sample Quantity
		Feldspar Dissolutio	Rock Fragment	Intergranular Dissolution Pore	Zeolite Dissolution Pore			
Wuqi	57.98	30.96	3.94	0.66	0.34	3.09	3.03	386
Dingbian	55.14	34.01	5.75	1.11	0.1	2.32	1.57	453

3.2. Reservoir Classification Evaluation

The dual-provenance system, a distinctive depositional system governed by bidirectional sediment supply, controls reservoir spatial configurations through a dual coupling mechanism of "sedimentary architecture-diagenetic modification". Its typical manifestation involves the development of composite fan-delta depositional systems (e.g., northwest–northeast oriented dual-lobe convergence) in multi-directional provenance convergence zones. The sedimentary mixing effect in these zones induces lithological heterogeneity and poor grain sorting, resulting in strongly heterogeneous reservoir substrates. During reservoir evolution, provenance differentiation exerts dual control: it governs diagenetic pathways through the spatial distribution of mineral components while simultaneously triggering fracture networks via stress concentration in tectonic transition zones. This creates a synergistic effect of differential cementation and permeability enhancement (by 2–3 orders of magnitude). The tripartite coupling mechanism of sedimentation–diagenesis–fracturing establishes provenance convergence zones as preferential targets for "sweet-spot" reservoir development, particularly demonstrating significant geological-engineering responses in tight reservoirs.

The dual-provenance system significantly intensifies reservoir heterogeneity and amplifies disparities in porosity–permeability parameters. The microscopic pore structure of the reservoir encompasses the geometric shape, size, distribution, connectivity, and proportion of pores and throats [30]. Mercury injection serves as an effective method for examining the reservoir's microscopic pore structure, enabling the extraction of pore throat characteristic parameters from the corresponding pressures on the mercury injection curve. While there are numerous types of pore throat structure parameters, they can be categorized into three groups that reflect the size, distribution, and connectivity characteristics of pores and throats. These three parameter categories, when combined appropriately, comprehensively depict the quality of the pore structure [31–33]. A statistical analysis was conducted on 151 rock samples from the Chang 6 reservoir in the Wuqi area to examine their pore throat structure parameters. When coupled with corresponding capillary pressure curve morphologies, this analysis led to categorizing Chang 6 oilfield into four types: Types I, II, III, and IV (Figure 3), with proportions of 21.9%, 41.1%, 27.8%, and 9.2%, respectively (Table 3).

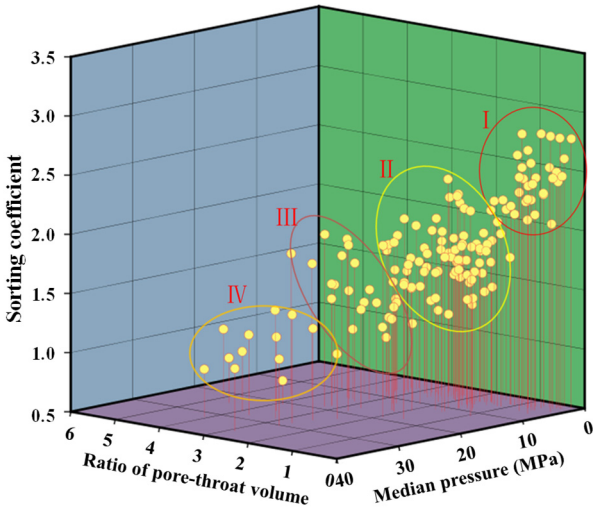


Figure 3. Correlogram of pore throat characteristic parameters of Chang 6 reservoir in Wu–Ding area, Ordos Basin.

Table 3. Classification and evaluation of Chang 6 reservoir by mercury injection coefficient and pore structure in Wu–Ding area.

Reservoir Classification	Sample Quantity	Porosity (%)	Permeability (mD)	Displacement Pressure (MPa)	Maximum Connected Throat Radius (μm)	Median Pressure (MPa)	Median Radius (μm)	Sorting Coefficient	Ratio of Pore Throat Volume	Maximum SHg (%)	Mercury Removal Efficiency (%)
I	33	13.8	2.049	0.46	2.31	3.51	0.28	2.41	0.64	80.92	38.30
II	62	12.9	0.584	1.08	0.82	7.46	0.15	1.76	2.11	73.11	29.97
III	42	11.5	0.213	1.68	0.58	10.65	0.11	1.47	2.76	69.15	23.45
IV	14	8.2	0.081	4.43	0.30	19.30	0.06	1.21	3.58	59.60	17.46
Average		12.9	0.686	1.42	1.03	8.58	0.16	1.77	2.11	72.46	28.82

Type I reservoirs exhibit low driving pressure, a wide range of pore distribution, diverse pore types, high proportions of large pores, a sorting coefficient generally greater than 2, and good connectivity. This type represents one of the most exceptional reservoirs in the study area in terms of reservoir performance and permeability. The average porosity is 13.8%, and the average permeability is 2.049 mD. Based on the test oil data, wells in this type of reservoir demonstrate an average daily oil production of 15.8 t/d with relatively low water content.

Type II reservoirs exhibit low-to-medium driving pressures, with pore distribution primarily concentrated in fine pores, moderate sorting, and high maximum mercury saturation. The average porosity is 12.9%, and the average permeability is 0.584 mD, indicating favorable reservoir performance and permeability. These reservoirs are widely developed in the study area and have been identified as key development areas. The test results show an average daily oil production of 11.6 t/d and a daily water production of 12.07 m^3/d.

Type III reservoir characteristics include the following: The driving pressure ranges from medium to high, featuring fine and small pore throats with a concentrated distribution, and moderate sorting. The average porosity of the reservoir is 11.5%, with an average permeability of 0.213 mD. This type of reservoir exhibits a predominantly microscopic pore structure, resulting in generally poor flow capacity. Test results indicate an average daily oil production of 6.74 t/d and a daily water production of 1.54 m^3/d.

Reservoir Type IV characteristics are as follows: Elevated driving pressure, reduced mercury saturation, fine and concentrated pore structure with minimal large pores, and poor sorting. The average porosity is 8.2%, while the average permeability is 0.081 mD. The reservoirs of this type exhibit inadequate storage performance and fluid flow capacity, rendering most of them ineffective as reservoirs.

Based on the statistical findings of reservoir distribution, the proportions of the four types of reservoirs in the Wuqi area are 26.3%, 41.3%, 25.0%, and 8.4%, whereas in the Dingbian area they stand at 16.9%, 40.8%, 31.0%, and 9.3%. It is evident that the percentages of Type I and II reservoirs in the Wuqi area significantly exceed those in Dingbian. Furthermore, the average porosity of northeastern sources in Wuqi measures at 12.85% with an average permeability of 0.642 mD, while for northwestern sources in Dingbian, these figures are recorded as 12.34% and 0.415 mD, respectively.

Integrated analysis of experimental data reveals distinct reservoir property variations controlled by provenance systems (Table 4), with critical geological implications. While the two areas show minimal porosity difference (Δ = 0.51%), permeability exhibits remarkable contrast—Wuqi's average permeability surpasses Dingbian's by 54.6%. The northeastern-sourced Wuqi reservoirs exhibit superior reservoir quality:

a. Higher proportion of premium reservoirs (Type I + II reservoirs: 67.6% vs. 57.7%).
b. Enhanced productivity with Type I reservoirs yielding 15.8 tonnes/day, contrasting Dingbian's 11.6 tonnes/day from Type II reservoirs.

Table 4. Comparison of physical properties of reservoirs from different sources.

Block	Porosity (%)	Permeability (mD)	Proportion of Type I + Type II Reservoirs	Proportion of Type III + Type IV Reservoirs
Northeast provenance (W area)	12.85	0.642	0.64	80.92
Northwest provenance (D area)	12.34	0.415	2.11	73.11

4. The Influence of Different Reservoir Pore Throat Structures

4.1. The Impact on Reservoir Properties

The microscopic structure of pore throats is an inherent factor influencing macroscopic reservoir properties. Through integration with corresponding capillary pressure curve morphologies, three key parameters—the selectivity coefficient, pore throat volume ratio, and median pressure—were chosen for correlation analysis. The correlation diagram between these parameters reveals their weak association with porosity but strong relationship with permeability—a reflection of specific characteristics within pores (Figure 4).

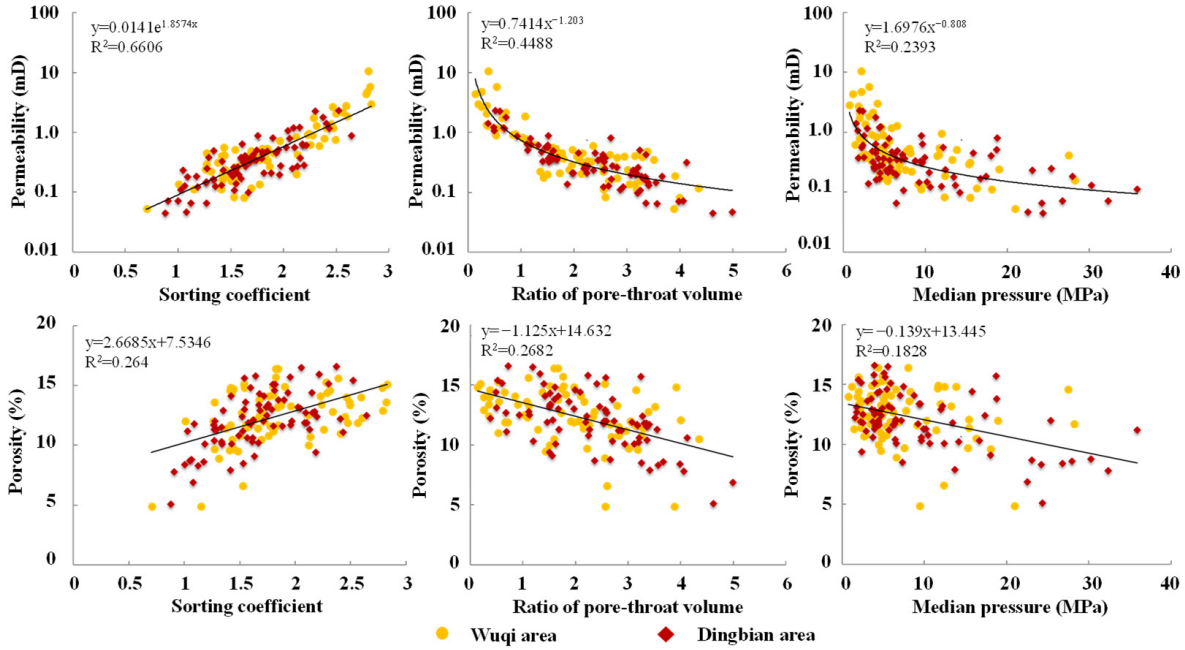


Figure 4. Correlations of pore throat characteristic parameters and physical properties of Chang 6 reservoir in Wu–Ding area, Ordos Basin.

This underscores how these structural factors exert greater influence on reservoir flow capacity than physical rock properties do [8]. Subsequent statistical analyses across various regions indicate Wuwei's broad spectrum in pore throat radius distribution, featuring predominantly dual or multiple high-frequency patterns; conversely, the D block exhibits primarily narrow single-type distributions—with dual/multiple types accounting for just 39%. Consequently, wider capillary radii correspond to increased larger channel proportions enhancing permeability, whereas higher uniformity signifies denser sedimentary rock formations [9]. A comprehensive assessment concludes that intense forces like compression and carbonate cementation impacted internal rocks in the D block, yielding singular chemical compositions and narrower porosity ranges and thereby diminishing overall permeability.

4.2. Analysis of Differences in Capacity Characteristics

The pronounced permeability anisotropy between dual-provenance systems exerts fundamental control on production dynamics within the Chang 6 reservoir. The statistical analysis of 156 production tests demonstrates significantly higher initial productivity in the W block (23.6 ± 3.2 m^3/d; composite water saturation 25.4 ± 4.1%) compared to the D block (15.8 ± 4.1 m^3/d; 17.7 ± 3.6% water cut) ($p < 0.01$, *t*-test). Our comparative petrophysical characterization of the Wuqi-W (NE thrust belt) and Dingbian-D (SW depression) tectonic units reveals critical reservoir architecture differences through integrated core analysis (n = 58 wells) and pore network modeling (Figure 5).

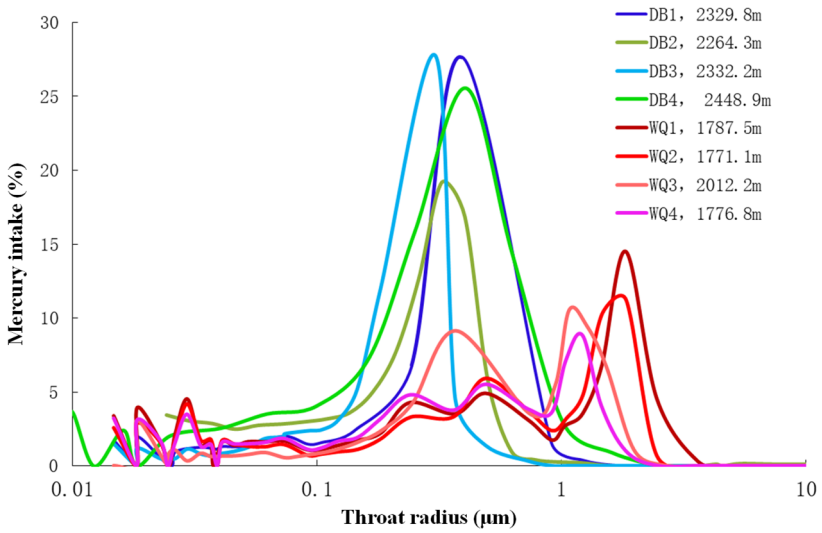


Figure 5. Statistics of distribution peak of pore throat radius in reservoir of Chang 6 reservoir in Wu–Ding area, Ordos Basin.

Quantitative evaluation shows comparable storage capacities (W: Φ = 12.16 ± 1.8%, K = 1.36 ± 0.42 mD vs. D: Φ = 12.38 ± 2.1%, K = 0.47 ± 0.23 mD) but distinct flow unit configurations. Mercury injection capillary pressure curves exhibit bimodal pore throat distributions in the W block (modal radii: 1.2 μm and 0.18 μm) versus unimodal distribution in the D block (modal radius: 0.25 μm), corresponding to a flow capacity contrast ratio of 2.9:1. This pore structure divergence directly impacts development efficiency:

a. The W block demonstrates a 73.2% effective displacement efficiency through optimized waterflood patterns (0.7 PV injected), sustaining 85% of initial productivity over a 12-month period.
b. The D block requires specialized stimulation (multistage fracturing + nanofluid imbibition) to achieve 42.1% recovery efficiency, with 58% production decline within the first 6 months.

The observed development challenges originate from provenance-controlled diagenetic modifications:

a. NW-derived volcanic lithics (W block: 15.7 vol%) promote chlorite coating preservation (8–12% coverage) inhibiting quartz cementation.
b. NE-sourced metamorphic fragments (D block: 6.3 vol%) enhance pressure dissolution, generating 18–22% tighter grain packing.

This study demonstrates that the characteristics of reservoir pore structure significantly control the oil production capacity and waterflooding development effectiveness during different water cut stages of oil wells. Research data reveals that during waterflooding development, reservoirs with large pore throats can establish an efficient displacement

system, maintaining high oil displacement efficiency even during the high-water-cut stage of 60% to 70%. In a typical example, block W, relying on its advantageous pore throat structure (with large pores accounting for 25.4%), maintains a 73% oil displacement efficiency even when the comprehensive water cut rises above 60%. In contrast, Block D, dominated by small pore throats, achieves only a 42% oil displacement efficiency due to difficulties in constructing an effective displacement system. This difference in seepage flow dominated by pore structure reveals the key control mechanism of pore throat radius distribution on oilfield development effectiveness.

5. Conclusions

(1) The Chang 6 reservoir in the Wu–Ding area of the Ordos Basin is characterized by well-sorted grains and moderate rounding. Kaolinite, chlorite, and calcite dominate its mineral composition. While the W and D blocks share similar petrological components, their contents differ significantly. Higher proportions of feldspar, clasts, and carbonate cementation in the D block enhance compaction and cementation, reducing original porosity. Residual intergranular and dissolution pores dominate the reservoir, with dissolution–intergranular and micro-pores being the primary pore types. The W block exhibits higher intergranular pore content and total specific pore volume than D block.

(2) Based on capillary pressure curves and pore throat parameters, the Chang 6 reservoir is classified into four structural types. Type I and II reservoirs, predominant in the W block's northeastern source system, feature low-to-moderate driving pressure, diverse throat sizes, high large-throat proportions, and favorable connectivity. Type III and IV reservoirs, with medium-to-high driving pressure and concentrated fine throats, show poorer mercury saturation and connectivity due to limited large pores.

(3) Permeability strongly correlates with pore throat structure parameters. The W block's reservoirs exhibit a broad, multi-peak throat distribution with higher large-pore proportions, enhancing flow capacity. In contrast, the D block's narrow, single-trough throat distribution restricts permeability. The proportion of large throats is critical in low-permeability reservoirs, directly influencing macroscopic flow dynamics.

(4) Microscopic pore structure significantly impacts reservoir productivity. The W block's high water saturation and liquid yield, coupled with stable production, reflect its abundant large pores, favoring water injection efficiency. Conversely, the D block's low water saturation, limited liquid yield, and rapid initial decline likely stem from narrow pore distribution and inadequate displacement pathways, hindering sustained production.

(5) Variations in lithology, compaction, and pore structure under diverse geological conditions directly affect reservoir permeability and hydrocarbon migration. Effective development strategies must account for these structural differences. Tailored well networks and injection–production methods should be optimized based on reservoir-specific characteristics to maximize resource recovery and operational efficiency.

Author Contributions: J.L. and M.W.: writing—original draft, and writing—review and editing, conceptualization. L.M.: funding acquisition, project administration. Y.L.: resources, data curation, formal analysis, methodology. K.Y.: visualization, validation, methodology, investigation, formal analysis. L.L.: data curation, project administration, conceptualization. All authors have read and agreed to the published version of the manuscript.

Funding: This research received no external funding.

Data Availability Statement: No new data were created or analyzed in this study.

Acknowledgments: Thanks to reviewers and editors for their careful review of this manuscript.

Conflicts of Interest: Authors Jun Li, Yan Li, Kaitao Yuan and Liang Liu were employed by the Dingbian Oil Production Plant of Yanchang Oilfield Company. The remaining authors declare that the research was conducted in the absence of any commercial or financial relationships that could be construed as a potential conflict of interest.

References

1. Zou, C.; Qiu, Z.; Zhang, J.; Li, Z.; Wei, H.; Liu, B.; Wang, X.; Chen, G.; Yang, F.; Liu, Y.; et al. Unconventional petroleum sedimentology: A key to understanding unconventional hydrocarbon accumulation. *Engineering* **2022**, *18*, 62–78.
2. Yao, J.; Deng, X.; Zhang, Y.; Hu, T.; Chen, M.; Pu, L. Characteristics of tight oil in Triassic Yanchang formation, Ordos Basin. *Pet. Explor. Dev.* **2013**, *40*, 161–169.
3. Sun, Z.; Zhu, H.; Jiang, T.; Xu, C.; Yang, X.; Liu, Q.; Wang, L.; Chen, Y.; Zhang, W.; Li, J.; et al. Decoding the complex fluvial-lacustrine sedimentary interactions: Insights from the Neogene Guantao Formation in the Bohai Bay Basin and Modern Poyang Lake, China. *Mar. Pet. Geol.* **2024**, *168*, 107007. [CrossRef]
4. Law, B.E.; Curtis, J.B. Introduction to unconventional petroleum systems. *AAPG Bull.* **2002**, *86*, 1851–1852.
5. Clarkson, C.R.; Jensen, J.L.; Blasingame, T.A. Reservoir engineering for unconventional gas reservoirs: What do we have to consider? In *SPE Unconventional Resources Conference/Gas Technology Symposium*; SPE: The Woodlands, TX, USA, 2011; p. SPE-145080.
6. Sun, L.; Zhu, R.; Zhang, T.; Cai, Y.; Feng, Z.; Bai, B.; Wang, D.; Liu, W.; Zhou, Q.; Chen, X.; et al. Advances and trends of non-marine shale sedimentology: A case study from Gulong Shale of Daqing Oilfield, Songliao Basin, NE China. *Pet. Explor. Dev.* **2024**, *51*, 1367–1385.
7. Pan, J.; Liu, S.; Yang, Y.; Liu, L.; Zhang, J.; Chen, D. Study progress of origin of fine-grained sedimentary rocks in deep-water area of lacustrine basin: Taking Yangchang Formation in Ordos Basin as an example. *Pet. Geol. Exp.* **2014**, *36*, 706–711.
8. Yang, J.; Yang, Y.; Dong, J. Sedimentation during the transgression period in late Triassic Yanchang formation, Ordos Basin. *Pet. Explor. Dev.* **2010**, *37*, 181–187.
9. Wang, Q.; Zhuo, X.; Chen, G.; Shi, J.; Wang, D. Diagenetic evolution and high-quality reservoir in Chang 6 sandstone in the western Ordos Basin. *Acta Pet. Sin.* **2005**, *26*, 17–23.
10. Zheng, R.; Wang, H.; Han, Y.; Wang, C.; Niu, X. Sedimentary facies characteristics and sandbody distribution of Chang 6 member in Jiyuan area of Ordos Basin. *Lithol. Reserv.* **2008**, *20*, 21–26.
11. Wei, W.; Azmy, K.; Zhu, X. Impact of diagenesis on reservoir quality of the lacustrine mixed carbonate-siliciclastic-volcaniclastic rocks in China. *J. Asian Earth Sci.* **2022**, *233*, 105265.
12. Gao, Y.; Wang, M.; Li, Y.; Jiang, Z.; Deng, Y.; Qin, J. Multi-scale pore structure characterization of lacustrine fine-grained mixed sedimentary rocks and its controlling factors: A case study of Lucaogou Formation in Jimusar Sag. *Energy Fuels* **2022**, *37*, 977–992. [CrossRef]
13. Mahmoodabadi, R.M. Assessment of linking diagenesis history to sequence stratigraphy evidences (systems tract), (a case study: Sarvak Formation in one of the super oil fields, SW, IRAN). *Carbonates Evaporites* **2023**, *38*, 59. [CrossRef]
14. Tong, Q.; He, D.; Xia, Z.; Huang, J.; Li, Y.; Xu, F.; Guo, S. Research on sand body architecture at the intersection of a bidirectional sedimentary system in the Jiyuan area of Ordos Basin. *Sci. Rep.* **2023**, *13*, 1226. [CrossRef]
15. Yao, J.; Liu, L.; Yang, Y.; Sun, H.; Zhang, L. Characterizing multi-scale shale pore structure based on multi-experimental imaging and machine learning. *Nat. Gas Ind. B* **2023**, *10*, 361–371. [CrossRef]
16. Zhao, C. Petrophysical Studies on Woodford Shale in Oklahoma and Wolfcamp Shale in Texas: A Multiple-Approach Methodology. Ph.D. Thesis, The University of Texas at Arlington, Arlington, TX, USA, 2022.
17. Guan, D.; Xu, X.; Li, Z.; Zheng, L.; Tan, C.; Yao, Y.; Guan, D.; Xu, X.; Li, Z.; Zheng, L.; et al. Current Status of Hydrocarbon Generation from Source Rocks Theory. In *Theory and Practice of Hydrocarbon Generation within Space-Limited Source Rocks*; Springer: Berlin/Heidelberg, Germany, 2017; pp. 19–68.
18. Zhen, Q.I.; Zhensheng, S.H.; Dazhong, D.O.; Bin, L.; Zhang, C.; Jie, Z.H.; Hongyan, W.A.; Xiong, B.; Zhenglian, P.A.; Hekun, G.U. Geological characteristics of source rock and reservoir of tight oil and its accumulation mechanism: A case study of Permian Lucaogou Formation in Jimusar sag, Junggar Basin. *Pet. Explor. Dev.* **2016**, *43*, 1013–1024.
19. Zou, C.; Zhang, G.; Yang, Z.; Tao, S.; Hou, L.; Zhu, R.; Yuan, X.; Ran, Q.; Li, D.; Wang, Z. Concepts, characteristics, potential and technology of unconventional hydrocarbons: On unconventional petroleum geology. *Pet. Explor. Dev.* **2013**, *40*, 413–428. [CrossRef]
20. Zhao, S.; Ding, R.; Tian, W.; Ye, J. Multiscale fine characterization of a coal pore-fracture system based on SEM, CT, and NMR in the Jingbian Block, Ordos Basin. *Energies* **2023**, *16*, 5315. [CrossRef]
21. Zhang, Z.; Liao, J.; Li, Z. Prediction of oil production in a tight sandstone reservoir: Triassic Chang 9 Member, Jiyuan Area, Ordos Basin, NW China. *Processes* **2024**, *12*, 382. [CrossRef]

22. Wang, K.; Guo, L.; Xu, C.; Wang, W.; Yang, T.; Lin, S.; Cai, Y. Multiscale characteristics of pore-fracture structures in coal reservoirs and their influence on coalbed methane (CBM) transport: A review. *Geoenergy Sci. Eng.* **2024**, *242*, 213181. [CrossRef]
23. Tohidi, E.; Hesan, M.; Azad, A.; Abbasi, M.; Sadeghnejad, S. Implementing pore size distribution into saturation height function modelling of reservoir rock types: A case study on a carbonate gas reservoir. *Gas Sci. Eng.* **2024**, *121*, 205188. [CrossRef]
24. Guo, T.; Li, X.; Ye, S.; Dong, X.; Wei, L.; Yang, Y. Theory and practice of unconventional gas exploration in carrier beds: Insight from the breakthrough of new type of shale gas and tight gas in Sichuan Basin, SW China. *Pet. Explor. Dev.* **2023**, *50*, 27–42.
25. Li, H.; Black, J.R.; Hao, Y.; Hao, P.; Mishra, A.; Haese, R.R. Modelling diagenetic reactions and secondary porosity generation in sandstones controlled by the advection of low-molecular-weight organic acids. *Basin Res.* **2024**, *36*, e12860.
26. Fu, J.; Li, S.; Liu, X.; Yang, S.; Luo, A.; Hui, X. Multi-layer composite accumulation mechanism and exploration significance of Jiyuan Oilfield, Ordos Basin. *China Pet. Explor.* **2013**, *18*, 1–9.
27. Liu, W.; Zhou, L.; Gao, S. Fracture characteristics of the Triassic Yanchang formation in the midwest of Ordos Basin. *Lithol. Reserv.* **2012**, *24*, 66–71.
28. Li, W.; Zhang, X.; Zhong, Y. Formation mechanism of secondary dissolved pores in arcose. *Oil Gas Geol.* **2005**, *26*, 220–223.
29. Huang, X.; Gao, H.; Dou, L. Mircro pore structure and water-flooding characteristics on tight sandstone reservoir. *J. China Univ. Pet.* **2020**, *44*, 80–88.
30. Yang, L.; Cheng, D.; Liu, B.; Bai, S. Reservoir classification and application based on mercury injection coefficient. *Sci. Technol. Rev.* **2014**, *32*, 46–50.
31. Li, Y.; Zhang, Z.; Zhang, C. Application of mercury injection data to Chang 6 reservoir classification in Changqing area. *Lithol. Reserv.* **2009**, *21*, 91–93.
32. Hu, M.; Shen, J.; Hu, D. Reservoir characteristics and its main controlling factors of the Pinghu Formation in Pinghu structural belt, Xihu Depression. *Oil Gas Geol.* **2013**, *34*, 185–191.
33. Zhao, J.; Liu, Z.; Xie, Q.; Zhou, J. Micro pore throat structural classification of Chang-7 tight oil reservoir of Jiyuan Oilfield in Ordos Basin. *China Pet. Explor.* **2014**, *19*, 73–79.

Disclaimer/Publisher's Note: The statements, opinions and data contained in all publications are solely those of the individual author(s) and contributor(s) and not of MDPI and/or the editor(s). MDPI and/or the editor(s) disclaim responsibility for any injury to people or property resulting from any ideas, methods, instructions or products referred to in the content.